J. of Supercritical Fluids 63 (2012) 46–51

Contents lists available at SciVerse ScienceDirect

The Journal of Supercritical Fluids

journal homepage: www.elsevier.com/locate/supflu

Neutron radiography on tubular flow reactor for hydrothermal synthesis: In situ monitoring of mixing behavior of supercritical water and room-temperature water

Seiichi Takami[a,*], Ken-ichi Sugioka[b], Takao Tsukada[b], Tadafumi Adschiri[a,c], Katsumi Sugimoto[d], Nobuyuki Takenaka[d], Yasushi Saito[e]

[a] Institute of Multidisciplinary Research for Advanced Materials, Tohoku University, 2-1-1 Katahira, Aoba-ku, Sendai 980-8577, Japan
[b] Department of Chemical Engineering, Tohoku University, 6-6-07 Aramaki, Aoba-ku, Sendai 980-8579, Japan
[c] WPI-Advanced Institute for Materials Research (WPI-AIMR), Tohoku University, 2-1-1 Katahira, Aoba-ku, Sendai 980-8577, Japan
[d] Department of Mechanical Engineering, Kobe University, 1-1 Rokkodai, Nada, Kobe 657-8501, Japan
[e] Department of Nuclear Science and Engineering, Research Reactor Institute, Kyoto University, 2 Asashiro-Nishi, Kumatori-cho, Sennan-gun, Osaka 590-0494, Japan

ARTICLE INFO

Article history:
Received 31 August 2011
Received in revised form 8 November 2011
Accepted 8 November 2011

Keywords:
Neutron radiography
In situ monitoring
Mixing
Tubular flow reactor
Water density
Hydrothermal synthesis

ABSTRACT

Neutrons are effectively scattered by hydrogen atoms and have high permeability in heavier elements including Fe, Cr, and Ni. Therefore, neutron radiography should enable the detection of differences in water density in a stainless-steel reactor. To test this, we performed neutron radiography on a tubular flow reactor for supercritical hydrothermal synthesis and visualized the mixing behavior of supercritical water and room-temperature water at a T-junction. The results showed that the difference in density between supercritical water and room-temperature water, as well as how the density changed during mixing, was clearly visualized. The partitioned flow in the side tube was also visualized while feeding room-temperature water. The results indicated the importance of buoyancy forces, as discussed by others in previous reports.

1. Introduction

Supercritical water is used in various chemical reaction processes including oxidation [1–3], hydrothermal synthesis of metal oxide nanoparticles [4–7], and chemical conversion of biomass and plastics [8–10]. Continuous flow reactors are applied for these processes by mixing several streams of reactants and water at supercritical conditions. Given the high reaction temperature and the properties of supercritical water as a reaction medium, the reaction rate can be quite fast. Therefore, rapid and uniform mixing of the streams is important to minimize the fluctuation of the products. For instance, the size and distribution of hydrothermally synthesized metal oxide nanoparticles are largely affected by how the reactants and supercritical water streams are mixed [11–13]. In order to visualize and understand the mixing of streams under supercritical conditions, various experimental and computational studies have been performed. In experimental studies, model fluids that mimicked the properties of water at supercritical conditions [14,15], transparent sapphire cells that allows optical observation of mixing at supercritical conditions [16,17], mesh grids in a tubular reactor that measured the conductivity distribution of fluid after mixing [18], and in situ X-ray diffraction measurements during hydrothermal synthesis [19] have been used to understand the mixing at supercritical conditions. Computer simulations have also been applied to study the flow dynamics of supercritical water [17,20–28]. Masuda et al. reported both numerical simulations and visualization experiments on T-junction mixing and found that natural convection was dominant in the flow tubes [17]. The relationship between the mixing behavior from numerical simulations and the size and shape of the products from experiments was also studied under various conditions including the shape of mixing components [20–25]. Although these methods provide various types of valuable information, there remain several problems, including difficulties in reproducing the real reactor shape that is used for the actual production of nanoparticles and in modeling the complicated behavior of water near the critical point and/or in the turbulent flow regime.

The scattering of neutrons has been utilized in various fields to visualize the internal structures of objects [29,30]. Although X-rays have higher permeability toward lighter elements, neutrons can penetrate materials with heavier elements and are mostly scattered by hydrogen atoms. Therefore, neutron radiography, that is,

* Corresponding author. Tel.: +81 22 217 6322; fax: +81 22 217 6323.
E-mail address: stakami@tagen.tohoku.ac.jp (S. Takami).

0896-8446/$ – see front matter © 2012 Published by Elsevier B.V.
doi:10.1016/j.supflu.2011.11.010

imaging of the internal structure of an object by measuring the scattered neutron intensity, is suitable for visualizing the density of water inside a tube or container composed of stainless steel or other alloys. Using neutron radiography, Peterson et al. have studied salt precipitation processes in supercritical water [31,32] and the flow pattern in a reverse-flow vessel for salt precipitation [33], and Balaskó et al. have revealed the behavior of supercritical water in a container [34]. In this study, we attempted to investigate the mixing of room-temperature water and supercritical water in a tubular flow reactor by neutron radiography. Such mixing should result in a decrease in temperature, and therefore, an increase in water density. We have previously studied the supercritical hydrothermal synthesis of metal oxide nanoparticles by using a tubular flow reactor and found that the mixing of the reactant and supercritical water plays a key role in controlling the size distribution of the resultant nanoparticles [11,12]. In this paper, we report the results of performing neutron radiography on the mixing of supercritical water and room-temperature water at a T-junction in a tubular flow reactor, which is almost identical in shape to the reactors used to synthesize metal oxide nanoparticles.

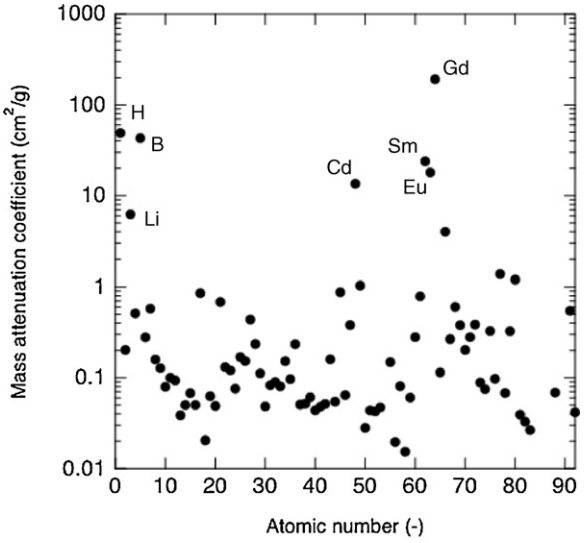

Fig. 1. Mass attenuation coefficient of thermal neutron for different elements.

2. Experimental

2.1. Supercritical hydrothermal reactor

In order to study the mixing behavior during supercritical hydrothermal synthesis, a tubular flow reactor with a T-junction [35–37] was used to mix a flow of heated water with a separate flow of water at room temperature. A high-pressure pump (Nihon Seimitsu Kagaku, NP-KX-540) supplied deionized water at a rate Q_{SC} of 4.0–8.0 g/min; this water was then heated by a furnace up to ca. 410 °C. A separate pump supplied deionized water at room temperature at a rate Q_{RT} of 0.0–20.0 g/min. In this study, we supplied water without adding metal ion precursors and did not perform hydrothermal reactions. The two flows were mixed at the T-junction, after which the mixed flow was then quenched by a jacket cooler and released from a back-pressure regulator (TESCOM, 26-1700 Series) that maintained the pressure at ca. 25 MPa. The T-junction was comprised of Swagelok and SUS316 tubes whose outer diameter and wall-thickness were 1/4 in. and 0.9 mm, respectively, and covered by a thermal insulator. The setup was almost identical to those we have used to synthesize metal oxide nanoparticles, except for the supplied fluid (water instead of metal ion solutions) and the diameter of the tubes (1/4-in. tube instead of the 1/8-in. tubes we have used in many cases). Table 1 shows the experimental conditions under which we obtained neutron radiography images. In these experiments, the supercritical water flowed downward while the room-temperature water was injected from the side of the T-junction.

2.2. Neutron radiography

Neutron radiography is an imaging technique in which a neutron beam is used to visualize the internal structure of objects. In this study, we used a thermal neutron beam emitted from the B4 port of the Kyoto University Reactor (KUR) at the Research Reactor Institute, Kyoto University. KUR was operated at 1 MW with a neutron flux of ca. 10^7 n/cm^2 s at the beam exit of the B4 neutron guide tube. Fig. 1 shows the mass attenuation coefficient for a thermal neutron as a function of atomic number [38]. Hydrogen, boron, and gadolinium have high mass attenuation coefficients and are therefore opaque against neutrons. In contrast, heavier elements including iron, nickel, and chromium are more transparent. Therefore, we can visualize the density of water inside the stainless-steel container by using a neutron beam. Fig. 2 shows a schematic of the experimental setup. The neutron beam passing through the mixing part was converted by a ^{6}LiF/ZnS scintillator screen (Fuji Electric Co. Ltd.) into luminescent light, which in turn was monitored by a charge-coupled device (CCD) camera (PIXIS-1024B, Princeton Instruments Co. Ltd.) equipped with a telephotographic lens that was deliberately located off of the neutron beam axis to avoid direct exposure to neutron irradiation. A square area of 6.0 cm × 6.0 cm around the mixing part was monitored by the CCD camera and converted into a 16-bit gray scale image with a resolution of 1024 × 1024 pixels. The typical period used to obtain a single image was 30 s. The obtained image was processed as described below.

2.3. Data analysis

We obtained 11 images, $I_i(x, y)$: $1 \le i \le 11$, $1 \le x, y \le 1024$, for each experimental condition. The images contained bright spots that randomly appeared as noise. Hence, we removed these spots as follows. From the ith (I_i) and ($i+1$)th (I_{i+1}) images, an image (I'_i) was produced where

$$I'_i(x, y) = \text{minimum}\{I_i(x, y), I_{i+1}(x, y)\} \quad \text{for} \quad 1 \le x, \quad y \le 1024 \qquad (1)$$

By summing the 10 images produced, we obtained a single image, $I(x, y)$, for each experimental condition. We performed the above procedure for experimental conditions with different flow rates and water stream temperatures, as shown in Table 1. The images

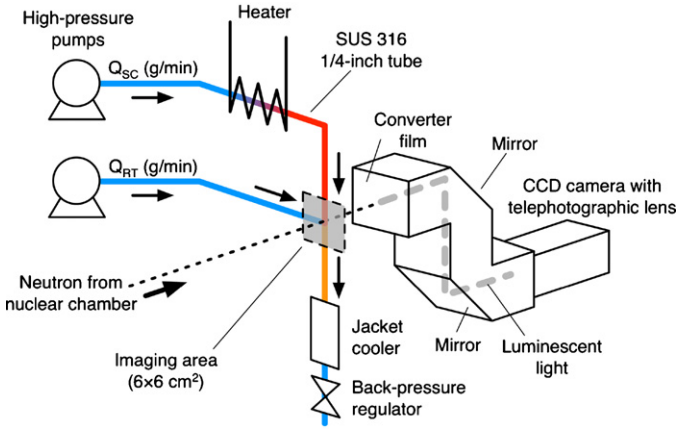

Fig. 2. Schematic of experimental setup.